THE
PHYSICAL REVIEW

A journal of experimental and theoretical physics established by E. L. Nichols in 1893

SECOND SERIES, VOL. 82, NO. 5 JUNE 1, 1951

Radiations from Yb^{169}

DON S. MARTIN, JR., ERLING N. JENSEN, FRANCIS J. HUGHES, AND R. T. NICHOLS
*Institute for Atomic Research and Departments of Chemistry and Physics, Iowa State College, Ames, Iowa**

(Received December 18, 1950)

The radiations from Yb^{169} have been examined by means of a thin lens spectrometer and absorption-coincidence techniques. The half-life was found to be 33±1.5 days. The half-life of the metastable state was determined as 0.67μ sec. Yb^{169} decays by electron-capture to Tm^{169}. Eleven gamma-rays were observed in the photoelectron and internal conversion spectra determined with the spectrometer. On the basis of the absorption-coincidence and spectrometer data, two decay schemes are discussed.

I. INTRODUCTION

A STUDY of the radiations of Yb^{169} has been carried out in this laboratory. It has included a determination of the electron and gamma-ray spectra by a thin lens beta-ray spectrometer and coincidence counting-absorption measurements. Although identification of eleven gamma-rays indicated that the decay scheme is complex, considerable information regarding the principal modes of decay has been obtained.

Bothe[1] first reported this activity as the component with the longest half-life (33d) in neutron irradiated ytterbium oxide. Since he identified Tm K x-rays by selective absorption, he proposed an assignment to isotope Yb^{169} with decay by orbital electron capture. On the basis of absorption curves he reported gamma-ray energies of 0.2 and 0.4 Mev. A shorter activity of about 100 hours was shown by Inghram, Hayden, and Hess[2] to belong to Yb^{175}, which decays by emission of β^-. Recently, Cork *et al.*[3] have reported beta-ray spectrometer measurements of the conversion electrons, listing nine lines. McGowan and DeBenedetti[4] in a systematic search for short-lived isomers reported a metastable state in the decay product, Tm^{169}, with a half-life of 1.0 μsec. The metastable state was reported from absorption measurements to be followed by electrons of 0.12 Mev (probably K-electrons from 0.19-Mev γ) and to be preceded by electrons of a 0.4-Mev gamma-transition as well as x-rays.

A one-gram sample of ytterbium oxide was supplied to us by Dr. F. H. Spedding and his co-workers for these and other studies. Effective separation from the light rare earths, including the elements samarium and europium, had been effected in ion exchange columns using Amberlite IR-100 ion exchange resin.[5] The ytterbium had then been further separated from the rare earths other than samarium and europium by repeated sodium amalgam reductions and extractions. Conditions for such extraction have been described extensively by Moeller and Kremers.[6] Lastly, the sample had been precipitated as oxalate, ignited to oxide and irradiated for one month in the Argonne National Laboratory pile. The decay of the radioactivity was followed by means of a hydrogen-filled G-M counter, and each count was compared with that of a uranium oxide counting standard. The decay of the electron fractions showed in addition to the 33-day component short-lived activities consistent with the 4.2-day Yb^{175} and the 7-day Lu^{176} in agreement with the work of Cork *et al.*[3] However, for a sample mounted with 450-mg/cm^2 aluminum before the counter to stop electrons, there was found to be no apparent deviation from a simple decay of 33±1.5 days which was followed over eight half-lives. Even so, some weak gamma-lines were associated with short-lived activity as noted by the spectrometer. Only radiations definitely associated with

* Work performed in the Ames Laboratory of the AEC.
[1] W. Bothe, Z. Naturforsch. **1**, 173 (1946).
[2] Inghram, Hayden, and Hess, Jr., Phys. Rev. **71**, 270 (1947).
[3] Cork, Keller, Rutledge, and Stoddard, Phys. Rev. **78**, 95 (1950).
[4] S. DeBenedetti and F. K. McGowan, Phys. Rev. **74**, 728 (1948).
[5] Spedding, Fulmer, Butler, Gladrow, Gobush, Porter, Powell, and Wright, J. Am. Chem. Soc. **69**, 2812 (1947).
[6] T. Moeller and H. E. Kremers, Ind. Eng. Chem., Anal. Ed. **17**, 798 (1945).

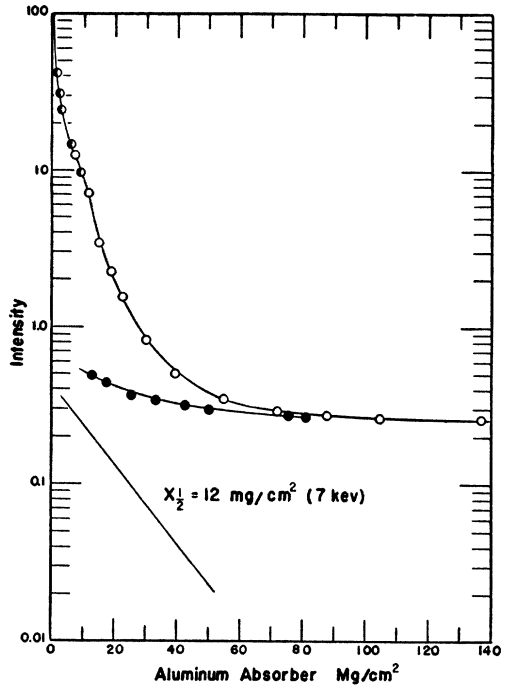

FIG. 1. Aluminum absorption curve for Yb^{169}. ⊙ Mica-window G-M counter. ◑ Windowless counter. ● Electrons removed by magnet.

the long-lived activity have been reported in this paper, and most measurements were performed after decay of the major fraction of the short-lived component.

Following the irradiation, the sample was dissolved in hydrochloric acid and processed through three sodium amalgam extractions. At least 99 percent of the activity was extracted and the absorption curves for the residue indicated that any radiation of significantly different character was certainly less than 0.1 percent of the original.

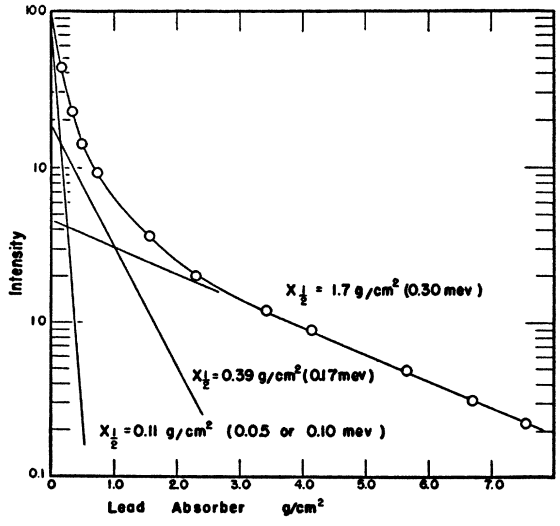

FIG. 2. Lead absorption curve for Yb^{169}.

An aluminum absorption curve of the radiation from Yb^{169} is presented in Fig. 1. A conventional end mica-window G-M counter was used for the high absorber values. The absorption curve from 0 to 9 mg Al/cm² was obtained with a windowless, flowing gas counter produced by the N. Wood Counter Laboratory of Chicago. The curves joined smoothly when an absorber equivalent to the window, air, and Cellophane sample cover was used. The flowing gas counter has proved effective in measuring the conversion electrons from a 25-kev isomeric transition with a half-life of 9 hours in Co^{58m}.[7] It should measure, therefore, the 40-kev Auger electrons that would be expected in about 10–15 percent of the K x-ray transitions. According to the range-energy curve of Glendenin[8] a counter with an air and window thickness of 4.0–4.5 mg/cm² should not detect with appreciable efficiency electrons with an energy of less than 60–80 kev. The absorption curve in Fig. 1 for the windowless counter indicated no exceedingly large group of electrons below that energy. The visual end point of the absorption curve of 80–90 mg Al/cm² would indicate a maximum electron energy of about 0.3 Mev. The absorption of photons in aluminum was also measured with electrons deflected by an Alnico permanent magnet so they could not enter the counter window. Tests with Co^{60} and Ce^{141} activities proved the arrangement effective for electrons of the energies involved. The resulting photon absorption curve is also included in Fig. 1. A soft component, which possessed a half-thickness of 11.8 mg Al/cm², was observed with an intensity about equal to the harder one. Since this corresponds to a photon energy of 7–8 kev, it is presumed to be the Tm L x-ray. Therefore, if the situation is normal in that the intensities of K and L x-ray transitions are not greatly different, the counter detection efficiencies for the 7.2-kev L x-ray and the 50.7-kev K x-ray must be approximately equal.† The main contribution to the electron count appears to fall into two groups, one with a range of about 80–90 mg/cm² and a more intense group with a range of 20–25 mg/cm² corresponding to an energy of 120–140 kev.

The characteristics of the photon component have been determined from the lead absorption curve shown in Fig. 2. An end-window brass counter tube was used. However, an aluminum absorber of 225 mg/cm² was placed immediately before the counter in all measurements. This aluminum would stop all conversion electrons and bring the secondaries into equilibrium with

[7] K. Strauch, Phys. Rev. **79**, 487 (1950).
[8] L. E. Glendenin, Nucleonics **2**, No. 1, 12 (1948).
† *Note added in proof:*—A referee has pointed out that the fluorescence yield for the L x-ray transition is significantly lower than the fluorescence yield of the K transition for which a value of 0.85 has been used. Therefore if the K and L transitions are equally probable, the radiative intensities are proportional to the respective fluorescence yields. Consequently the counter efficiency for the L x-rays is probably somewhat greater than for the K x-rays. This brings the counter efficiencies more in line with the curves of reference 17 but does not change other arguments in this paper.

the primary radiation of interest (30 kev–300 kev). The hardest component, half-thickness of 1.72 g Pb/cm², corresponding to an energy of 0.30 Mev, possessed an intensity of 5 percent. An intermediate component with a half-thickness of 0.39 g Pb/cm² would correspond to an energy of about 0.17 Mev, and it had an intensity of 19 percent. The softest component corresponding to 76 percent cannot be assigned an unambiguous energy value, because it falls in the vicinity of the lead K absorption edge. However, the very high absorption coefficient of most the radiation in Sn, as seen in Fig. 3, indicates that by far the largest fraction of the soft radiation has an energy of about 50–55 kev rather than the 100–110 kev. The soft radiation presumably consisted mostly of the 50-kev Tm K x-radiation and was present in very high counting intensity compared to the gamma-counting rates.

II. THIN LENS SPECTROMETER AND MEASUREMENTS

A. Experimental Arrangement

The radiations from the irradiated ytterbium were examined by means of a thin lens beta-ray spectrometer which has been described previously.[9] The resolution of the spectrometer was 2.1 percent (half-width) except for the inserts shown in Fig. 5, in which case the resolution was somewhat better in order to resolve the lines. Except for curve A of Fig. 6 all the data were obtained with a G-M counter in which the window was a Formvar film having a cutoff at about 15 kev. For curve A of Fig. 6 the window was a much thinner Formvar film supported on a grid. This window had a cutoff at about 5 kev. The spectrometer was calibrated by means of the F conversion line of ThB (1385 $H\rho$) and the annihilation radiation from Zn^{65}. The energies of the gamma-rays have been calculated from the peaks of the lines after applying corrections for the earth's magnetic field, the resolution of the spectrometer, and the surface density of the source.[9]

B. Internal Conversion Spectrum

The internal conversion source, which was grounded, had a surface density of about 7 mg/cm² and was mounted on a polystyrene—Formvar film having a surface density of about 40 micrograms/cm². The internal conversion spectrum is shown in Fig. 4. As can be seen from the figure, there are no beta-particles emitted in the decay of Yb^{169}. The energies of the gamma-rays, as determined from this spectrum, are listed in Table I as conversions in Tm, since the decay is by electron-capture. Conversion lines from eight gamma-rays were observed. In addition, the hump at about 680 gauss-cm, which is labeled $K_\alpha(L)$, is consistent with the energy of Auger electrons from Tm.

[9] Jensen, Laslett, and Pratt, Phys. Rev. 75, 458 (1949).

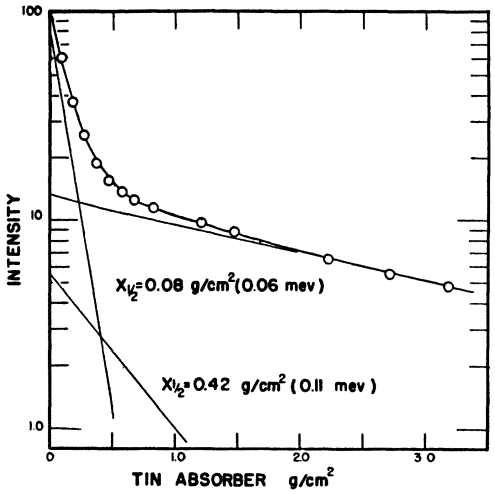

FIG. 3. Tin absorption curve for Yb^{169}.

C. Photoelectron Spectrum

Figure 5 shows the spectrum produced by photoelectrons ejected from a lead foil, having a surface density of 39.3 mg/cm², which was fastened to an aluminum cap covering the source. The lines shown in Fig. 5 can be ascribed to the characteristic x-rays from Tm, due to electron-capture and internal conversion, and six gamma-rays, five of which are also shown in the internal conversion spectrum of Fig. 4. The energies of the gamma-rays and x-rays, as determined from Fig. 5, are listed in Tables I and II respectively as conversions in Pb.

The low energy end of the photoelectron spectrum was also determined by means of a Ag foil having a surface density of 54.0 mg/cm². This photoelectron spectrum is shown by curve B of Fig. 6. In order to determine more definitely the conversion shell of these lines the spectrum was also determined with an In foil having a surface density of 24.3 mg/cm². The data shown by curve A in Fig. 6 were obtained with a more intense source and a G-M counter window having a cutoff at about 5 kev. Figure 6 shows two additional

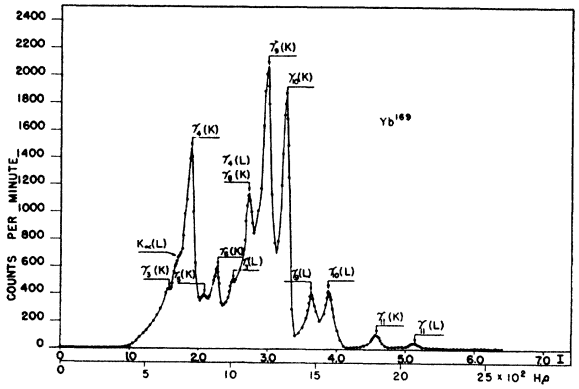

FIG. 4. Internal conversion spectrum for Yb^{169}.

TABLE I. Gamma-ray energies of Yb^{169}.

Gamma-ray	Electron energy (corrected) kev	Conversion shell	Gamma-ray energy kev	Relative weight	Average energy kev
1	19.4	Ag(L)	22.6	4	
	22.6	Ag(M)	23.3	2	22.8
2	38.3	Ag(K)	63.8	10	
	35.7	In(K)	63.6	10	63.7
3	34.2	Tm(K)	93.5	3	
	85.6	Tm(L)	94.8	3	
	68.7	Ag(K)	94.2	3	
	67.5	In(K)	95.4	3	94.5
4	50.5	Tm(K)	109.8	10	
	100.5	Tm(L)	109.7	5	
	85.2	Ag(K)	110.7	10	
	83.0	In(K)	110.9	10	110.4
5	60.4	Tm(K)	119.7	5	
	96.2	Ag(K)	121.7	3	120.4
6	71.4	Tm(K)	130.7	10	
	46.4	Pb(K)	134.4	10	
	107.3	Ag(K)	132.8	10	
	104.7	In(K)	132.6	10	132.6
7	54.6	Pb(K)	142.6	3	142.6
8	72.2	Pb(K)	160.2	3	
	100.5	Tm(K)	159.8	5	160.0
9	119.2	Tm(K)	178.5	10	
	168.2	Tm(L)	177.4	5	
	90.1	Pb(K)	178.1	10	
	162.9	Pb(L)	176.6	5	177.9
10	139.5	Tm(K)	198.8	10	
	188.6	Tm(L)	197.8	5	
	110.3	Pb(K)	198.3	10	
	182.8	Pb(L)	196.5	5	
	196.7	Pb(M)	200.5	2.5	198.3
11	248.1	Tm(K)	307.4	10	
	298.9	Tm(L)	308.1	5	
	220.6	Pb(K)	308.6	10	
	294.0	Pb(L)	307.7	5	308.0

gamma-rays that were not observed in either the internal conversion spectrum of Fig. 4 or the photoelectron spectrum of Fig. 5. The gamma-ray and x-ray energies as determined from Fig. 6 and the photoelectron spectrum obtained with the In foil, are listed in Tables I and II, respectively, as conversion in Ag or In as the case may be.

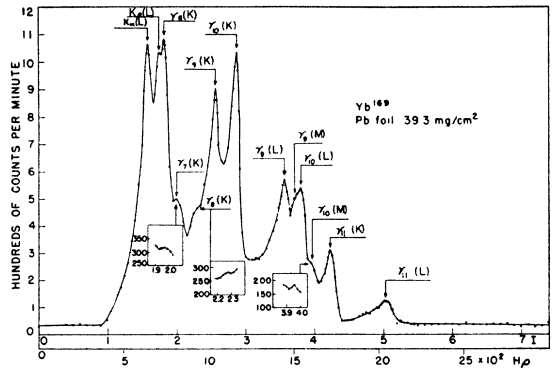

FIG. 5. Spectrum of photoelectrons from a lead foil for Yb^{169}.

In calculating the energies given in Tables I and II the binding energies of the K shells were determined from the critical absorption wavelengths.[10] These values are 88.0, 59.3, 27.9, and 25.5 kev, respectively for Pb, Tm, In, and Ag. The binding energies of the L shells are average experimental values determined from the differences between a number of K and L lines for the respective metal foils. These values are 13.7, 9.2, 3.4, and 3.2 kev, respectively for Pb, Tm, In, and Ag.

The average energies given for the K_α and K_β x-rays in Table II are in good agreement with those given by Compton and Allison,[11] namely, 50.7 kev and 49.8 kev, respectively, for $K_{\alpha 1}$ and $K_{\alpha 2}$, and 57.6 kev for $K_{\beta 1}$. This serves as an excellent check on the calibration of the spectrometer.

Eleven gamma-rays were found for Yb^{169}. Gamma-rays 1, 7, and 8 listed in Table I are in addition to those

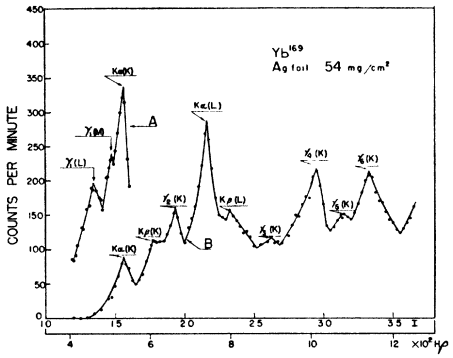

FIG. 6. Spectrum of photoelectrons from a silver foil for Yb^{169}. Curves A and B were obtained with G-M counters with window thicknesses of 0.3 mg/cm² and 0.03 mg/cm², respectively.

given by Cork *et al.*[3] The energy values of the other gamma-rays listed in Table I are in good agreement with those of Cork *et al.* The probable error of the gamma-ray energies given in Table I is estimated to be less than one percent.

D. Intensities of Gamma-Rays and Internal Conversion Electrons

Approximate relative values of the intensities of the gamma-rays and the internal conversion electrons can be obtained from the maximum counting rate of the respective lines. In the case of Figs. 5 and 6 the spread in momentum, owing to the surface densities of the Pb and Ag foils, was greater than the momentum spread which the spectrometer could accept.[9] In this case, *neglecting scattering*, the maximum counting rate for any line is proportional to the number of such quanta

[10] A. H. Compton and S. K. Allison, *X-Rays in Theory and Experiment* (D. Van Nostrand Company, Inc., New York), second edition, p. 791.

[11] Reference 10, p. 784.

emitted by the source, the photoelectric absorption coefficient, the transmission of the counter window and inversely proportional to the spread in momentum produced by the metal foils. The photoelectric absorption coefficients were calculated by means of Gray's[12] empirical formula and the spread in momentum produced by the metal foils by means of a formula given by Heitler.[13] The internal conversion spectrum was treated in a similar manner. Relative intensities have been calculated with respect to gamma-ray 9. Table III gives the approximate relative intensities of the more prominent gamma-rays (q_i/q_9) and internal conversion electrons (e_i/e_9). Where the gamma-ray lines are fairly well separated, these ratios may be in error by a factor of about two.

III. COINCIDENCE MEASUREMENTS

A. Experimental Arrangement

Coincidence counting experiments employing G-M counters with 2.2–2.8-mg/cm² mica windows were perTABLE II. X-ray energies of Tm.

X-ray	Electron energy (corrected) kev	Conversion shell	X-ray energy kev	Relative weight	Average energy kev
K_α	35.3	Pb(L)	49.0	10	
	25.1	Ag(K)	50.6	10	
	47.3	Ag(L)	50.5	10	
	23.0	In(K)	50.9	10	
	47.3	In(L)	50.7	10	50.3
K_β	42.3	Pb(L)	56.0	3	
	32.1	Ag(K)	57.6	5	
	54.5	Ag(L)	57.7	3	
	29.8	In(K)	57.7	5	
	54.5	In(L)	57.9	3	57.4

formed. The counters had separate high voltage supplies. A block diagram of the electronic arrangement is shown in Fig. 7. As shown in the diagram, the pulses in channel 2 could be applied immediately to the grid of a mixer tube or sent first to a delay circuit which was based on a design by Watts *et al.*[14] This circuit provided a delay of from 2.4 to 20 μsec. By selector switches a choice of gate widths from 0.8 to 1.5 μsec could be obtained for each channel. Pulses were observed on a synchroscope with sweep speeds of 2 or 6 μsec/inch. The sweep was calibrated frequently by an oscillator tuned to the fifth harmonic of a 100 kc crystal, which served as the time scale. The delay time could be read from the scope together with the pulse widths or gates, τ' and τ'' for the separate channels. In the subsequent treatment the following symbols and conventions have been used.

Superscripts (′) and (″) refer to channel or counter 1 and 2, respectively. Numeral subscripts refer to the transition as indicated in Tables I and II. Subscript "d" indicates a coincidence counting rate with the pulse in channel 2 delayed.

Subscript "c" indicates a coincidence counting rate with no delay.

t_d = time in microseconds that pulse was delayed in channel 2.

$t_{\frac{1}{2}} = 0.693/\lambda$ = half-life of metastable state in microseconds.

e = an electron component (internal conversion or Auger electrons).

q = a photon component.

α = a gamma-ray conversion coefficient = e/q.

n = number of transitions or disintegrations per unit time.

C = a counting rate.

E = a counter efficiency for detecting a radiation particle or photon emitted by the sample.

Preceding radiation = the radiation which precedes the metastable state.

Delayed radiation = radiation which follows the metastable state.

Parallel radiation = radiation from disintegrations which do not pass through the metastable state.

TABLE III. Approximate relative intensities of the gamma-rays and internal conversion electrons from Yb^{169}.

Gamma-ray	q_i/q_9	e_i/e_9
2	1.3	
4	2.1	4
6	2.0	0.4
9	1.0	1.0
10	1.7	0.8
11	0.6	0.03
K_α x-ray	9.8*	

* Average from the $K_\alpha(L)$ photoelectrons in silver and in lead.

Accidental coincidences are obtained due to the finite gates and would normally be given by:

$$\text{Accidental rate} = (\tau' + \tau'')C'C''. \quad (1)$$

Experimentally determined accidental rates obtained by the use of separated samples for various permutations of the gate widths gave good agreement with values of τ' and τ'' read from the synchroscope. When necessary, the accidentals for delayed counts were computed as indicated by DeBenedetti and McGowan[4] to correct for accidentals missed because of true coincidences. The computed accidental coincidence rate together with the coincidence background, determined for the various counter arrangements employed, were subtracted from each coincidence count also.

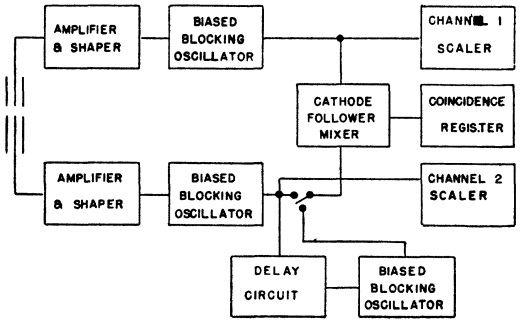

FIG. 7. Block diagram of coincidence circuit.

[12] L. H. Gray, Proc. Cambridge Phil. Soc. **27**, 103 (1931).

[13] W. Heitler, *The Quantum Theory of Radiations* (Oxford University Press, New York, 1944), second edition, p. 219.

[14] R. W. Watts, Manhattan District Report MDDC 741 (unpublished).

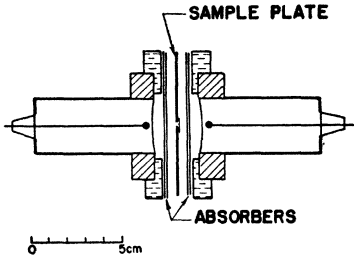

FIG. 8. Coincidence counter arrangement.

The counter arrangement is shown to scale in Fig. 8. Each counter was supported in a Lucite mount so that absorbers could be inserted between the counter and sample in a manner very similar to the conditions under which the absorption curves in Figs. 1–3 were obtained. The sample was prepared by evaporation of a small drop of $YbCl_3$ solution on mica of about 1 to 2 mg/cm^2 thickness. The mica was supported on a brass plate $\frac{1}{16}$ inch thick, directly in front of a hole with a 3-mm diameter. The bare sample faced counter 1. The brass plate was found necessary to minimize the scattered radiation which passed from one counter to the other. Its effectiveness in preventing this was evidenced by an experiment in which an equilibrium $Sr^{90}-Y^{90}$ sample was counted in this arrangement. Each of these isotopes decays by β^- emission without a gamma.[15] The ratio of coincidences to individual counts obtained was $C_c/C''=1.2\times10^{-3}$. A quantity of this magnitude could be expected to result from coincidence of bremsstrahlung radiation with electrons and is very small compared with the measured $(e-e)_c$ coincidence rates observed with the Yb^{169} samples.

The counter arrangement gave the maximum geometry possible for each counter with a nearly symmetric arrangement and permitted the use of absorbers under the nearly standard conditions of radiochemists for analyzing the radiation counted. Attainment of maximum counting efficiency is of considerable importance since coincidence counting rates are usually low, and long times are required to get results of statistical significance. In general, individual counting rates were maintained less than 7000 counts/min to avoid rapid deterioration of the counter tubes and eliminate excessive losses due to counter dead times which were estimated to be about 250 microseconds.

The operation of the delay circuit was checked by counting a sample of Co^{60} of the maximum intensity employed with a minimum delay setting. No counts in excess of the accidentals were obtained.

The resolving time of the coincidence register was determined from the counting losses incurred with each channel operating on the same counter. It was found to be 0.093 second. In the few cases where significant, the coincidence rates were corrected for these losses. However, intensities were always used so that such corrections were not greater than 5 to 6 percent.

It has been assumed in the treatment that the efficiency of the counters can be separated into factors in the manner:

$$E_i=\omega A_i\epsilon_i, \tag{2}$$

where ϵ is the intrinsic efficiency for counting a particular radiation which penetrates the counter, A is the absorption (and scattering) factor of absorber material placed between the sample and counter, and ω is the effective solid angle or geometry factor. Such a treatment is believed to be valid within the low accuracy of the coincidence measurements resulting from statistical fluctuations. ϵ is very nearly equal to one for an electron penetrating the G-M counter window. ϵ for photons of low energy (<0.5 Mev) is of the order of 10^{-3} to 10^{-2}, but reliable values have not been satisfactorily determined for energies of interest, i.e., 7 to 300 kev. Values of ω' and ω'' were determined with samples of Co^{60} and Au^{198}. For example, ω' was obtained from the coincidence counting rate between electrons and photons measured when the aluminum absorber before counter 2 was sufficient to stop all electrons. A small correction was necessary for the $(q-q)_c$ coincidence rate. Thus, for both the Co^{60} and Au^{198}

$$\omega'=\lim_{A'\to1}(e'-q'')_c/q''=0.115, \tag{3}$$

Since ω' was the largest possible efficiency for the detection of any radiation particles in counter 1, the losses in counting rates caused by two radiation particles from the same disintegration passing through the same counter were small. Similarly, ω'' was found to be 0.135.

With the conventional mica window counters employed, the air-window equivalent for counter 1 amounted to an absorber thickness 3.5 to 4.0 mg/cm^2. For counter 2 it was 4.5 to 5.5 because of the additional mica sample mount. Of the major peaks shown in Fig. 4 the Auger electrons, e_x, and the conversion electrons e_{4K} and e_{6K}, were certainly not counted, since effective counting efficiencies for these windows would be obtained only for energies greater than 80 kev. Higher energy electrons including the e_{4L} were counted effectively. Apparently, the greatest contribution to the counting rate was the e_{9K} and e_{10K}. This discrimination against the e_{4K} and e_{6K} proved very useful for the interpretation of coincidence data.

B. Decay Period of the Metastable State

The $(e-e)_d$ coincidence rate was measured over the maximum delay time range possible with the equipment. If $(e-e)_{d-\text{obs}}$ represents the observed number of delay counts which occurred per unit time with a particular setting of the instrument, the total delay coincidence rate $(e-e)_{d-\text{tot}}$ would be defined in the

[15] L. E. Glendenin, NNES-PPR **9B**, Paper No. 7.11.2 (1946); L. E. Glendenin and C. D. Coryell, NNES **9**, Paper 78 (1950). [Reported in G. T. Seaborg and I. Perlman, Revs. Modern Phys. **20**, 585 (1948).]

equation:

$$(e-e)_{d-\text{obs}}=(e-e)_{d-\text{tot}}\lambda\int_{t_d-\tau'}^{t_d+\tau''}e^{-\lambda t}dt$$

$$=(e-e)_{d-\text{tot}}[e^{\lambda\tau'}-e^{-\lambda\tau''}]\exp(-\lambda t_d). \quad (4)$$

Thus for constant gates the observed counting rate decreases exponentially with delay time. The experimental curve is shown in Fig. 9. Individual times could certainly not be measured with an accuracy of better than ± 0.1 μsec. A least squares treatment gives a half-life of 0.67 μsec. The half-life depends upon only the slope of the curve and is therefore independent of the time required to trigger the sweep of the synchroscope. This value does appear to be significantly lower than the 1.0 μsec of DeBenedetti and McGowan.[4] In a recent progress report McGowan[16] has indicated a half-life of 0.75 μsec, presumably determined by means of scintillation counters and delay-line techniques. This revised half-life is certainly in satisfactory agreement with our value.

C. Coincidence Absorption Curves

The coincidence counting rate with no delay was measured with no absorber before counter 1 and various aluminum absorbers before counter 2. Results have been plotted in Fig. 10. With no absorber before either counter the main contribution is due to $(e-e)$ coincidences. With 225 mg Al/cm^2 before counter 2, the count is due to the $(e'-q'')_c$, of which the largest component is $(e'-q_K'')_c$. For the curve in Fig. 10 giving $(e-e)_c$ it was necessary to subtract the estimated $(e'-q'')_c+(q'-e'')_c$ contributions from the coincidence rate. This component for no absorber was estimated to be four times the $(e'-q'')_c$ rate for the 225-mg Al/cm^2 absorber, since it contains the $(q_K'-e'')_c$, the $(e'-q''_L)_c$,

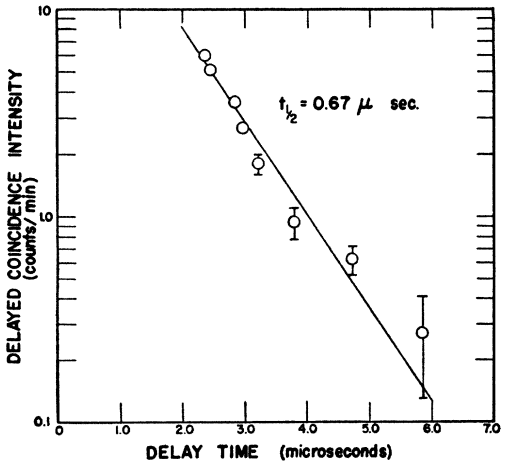

FIG. 9. Decay curve of metastable state in Tm^{169}.

[16] F. K. McGowan, AEC Report ORNL 694, p. 20 (1950), unpublished.

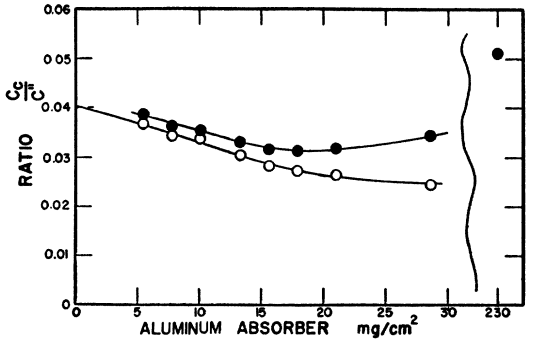

FIG. 10. Aluminum absorption curve for immediate coincidences. ● Total counting rate. ○ Electron component only.

and $(q_L'-e'')_c$, all of about equal magnitude. For intermediate absorbers the $(q_K'-e'')_c$ and $(q_L'-e'')_c$ components were assumed to be proportional to e'' and the $(e'-q_L'')_c$ fraction proportional to the absorption factor for the L x-ray calculated with an 11.8-mg/cm^2 half-thickness. For the channel gates employed, about one-half of the total delays were counted with the immediate coincidences. It was shown in the subsequent experiment that the contribution of delays to the $(e-e)_c$ coincidence was about 5 percent. However, a large fraction of $(e'-q'')_c$ was actually due to delays between preceding radiation including the original K x-ray accompanying the orbital capture and the conversion electrons following the metastable state.

Coincidence counting rates were also obtained with the pulses on the No. 2 channel fed through the minimum setting of the delay circuit. With the gates used, delays between 0.99 and 3.52 μsec were counted which would mean that on the basis of the 0.67-μsec half-life, 33 percent of the total delays were counted. The absorption curves obtained in these experiments are shown in Fig. 11. Thus, the curve with the absorber before counter 1 represents the absorption characteristics of the delayed radiation, and the curve with the absorber in front of counter 2 represents the absorption characteristics of the preceding radiation.

IV. DECAY SCHEME

Attempts to describe a decay scheme for the principal modes of decay of Yb^{169} which are quantitatively consistent with the intensities from the spectrometer and the coincidence counting rates have been only partially successful. A number of features, however, have been definitely established and are included in the following. Certainly transitions 1, 3, 5, 7, or 8 could not have offered appreciable contributions to the counting rates. The low intensity transition 11 would have been important with thick absorbers, since it was the hardest component. Several qualitative features of the decay scheme are indicated by the coincidence counting rates.

First, the $(e-e)_c/e''$ ratio, illustrated in Fig. 10, is 0.040 when extrapolated to zero window thickness. A comparison with the value of 0.115 for ω' indicates that

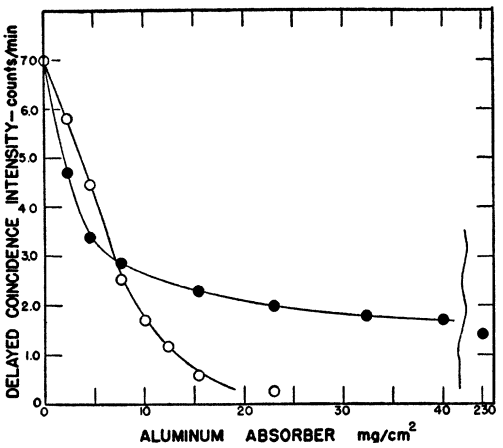

FIG. 11. Aluminum absorption curve for delayed coincidences. ○ Absorber before counter 1-delayed radiation component. ● Absorber before counter 2-immediate radiation component.

most of the electrons counted must be associated with two or possibly more highly internally converted transitions which are in immediate cascade, i.e., which are not separated by the metastable state. Since only L electrons were counted for transitions 4 and 6, it follows that the 9 and 10 electrons must be the ones which are in immediate cascade. The negative slope of the $(e-e)_c/e''$ ratio with absorber thickness appears to be real. The very high electron–electron coincidence rate appears to eliminate the decay scheme proposed by Cork *et al.*,[3] in which alternative cascades of 9 and 6, 10 and 4, or 11 can occur, although the energies of each path are within the precision of the spectrometer.

The difference in the absorption curves of the preceding and delayed radiation is also important. Thus, the delayed radiation is essentially an electron component with absorption characteristics similar to those of the total radiation. A thickness of 20 mg Al/cm² sufficed to reduce the delayed radiation nearly to zero. On the other hand, the delayed coincidence rate with 230 mg Al/cm² for the preceding radiation amounted to 20 percent of that for zero absorber, indicating a hard component. This hard component consists of the gamma-ray photons and K x-rays associated with the orbital capture or the internal conversion process that might precede the metastable state. However, the electron component of the preceding radiation is softer than the total electron. Moreover, $C_{d-\text{tot}}/C''$ was 0.0040, indicating that the delayed cascade of counted conversion electrons was only about 5 percent of the immediate cascade. (With the gates employed, 0.5 of the delays were counted in the experiments of no delay.) A correction was therefore applied to the limiting value of the ratio:

$$\lim_{A''\to 1}(e-e)_c/e''=0.040-0.002=0.038.$$

The ratio obtained with 230 mg Al/cm² for $(e'-q'')_{d-\text{tot}}/q''$ was 0.051. Again this represents a very high value by comparison to ω' and indicates that most of the electrons counted must have followed the metastable state. It also makes the possibility of decay directly to the ground state of Tm^{169} appear very unlikely.

Decay scheme A, which is shown in Fig. 12, is consistent with the gamma-ray energies and intensities obtained from the spectrometer data as listed in Tables I and III. The branching ratios were estimated from the gamma-ray and conversion electron intensities with the aid of the L photoelectrons produced from the lead foil by the Tm K x-rays. Relative intensities per transition and some conversion coefficients based on these branching ratios have been included in Table IV.

This decay scheme agrees qualitatively with the conclusions given previously from the coincidence experiments. A further quantitative test was made by computing some coincidence counting ratios. In all the computations that follow, several terms contributing less than 5 percent to the counting rates have been omitted for simplicity. This is consistent with the accuracy of the coincidence data. Since only the L electrons of γ_4 were counted, the channel 2 electron counting rate extrapolated to zero window is given by

$$\lim_{A''\to 1}e''=\left[\left(\frac{n_4\alpha_{4L}}{1+\alpha_4}+\frac{n_9\alpha_9}{1+\alpha_9}+\frac{n_{10}\alpha_{10}}{1+\alpha_{10}}\right)\omega''-\frac{n_9\alpha_9\alpha_{10}(\omega'')^2}{(1+\alpha_9)(1+\alpha_{10})}\right]. \quad (5)$$

The last term represents the largest of several corresponding to the loss of counts because of two electrons in cascade penetrating the same counter. Using the data of Tables III and IV and the spectrometer e_{4K}/e_{4L} ratio of 12 makes this expression

$$\lim_{A''\to 1}e''=n_9\omega''(0.92-0.13\omega''). \quad (6)$$

The expression for the electron–electron coincidences is

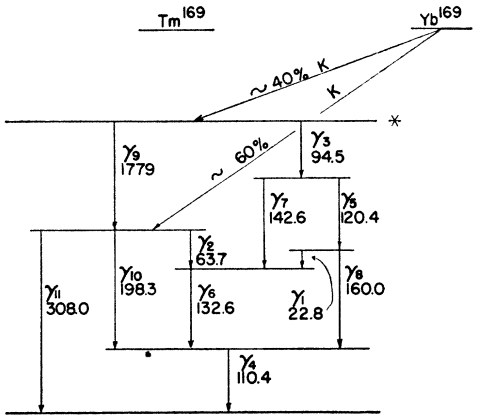

FIG. 12. Decay scheme A. The energies are given in kev.

given by

$$(e-e)_c=n_9\left[\frac{\alpha_9\alpha_{10}(E_9'E_{10}''+E_{10}'E_9'')}{(1+\alpha_9)(1+\alpha_{10})}+\frac{\alpha_9\alpha_{4L}(E_{4L}'E_9''+E_9'E_{4L}'')}{(1+\alpha_9)(1+\alpha_4)}+\frac{n_{10}\alpha_{10}\alpha_{4L}(E_{4L}'E_{10}''+E_{10}'E_{4L}'')}{n_9(1+\alpha_{10})(1+\alpha_4)}\right]. \quad (7)$$

With the counter efficiencies employed, coincidence losses caused by two cascade particles in the same counter can be ignored. Extrapolation to zero window for counter 2 yields:

$$\lim_{A''\to 1}(e-e)_c=n_9\omega'\omega''\left[\frac{\alpha_9\alpha_{10}(A_9'+A_{10}')}{(1+\alpha_9)(1+\alpha_{10})}+\frac{\alpha_9\alpha_{4L}(A_9'+A_{4L}')}{(1+\alpha_9)(1+\alpha_4)}+\frac{n_{10}\alpha_{10}\alpha_{4L}(A_{10}'+A_{4L}')}{(1+\alpha_{10})(1+\alpha_4)n_9}\right]. \quad (8)$$

A_{4L}', A_9' and A_{10}' were assumed to be 0.7, 0.75, and 0.75, respectively. With these the computed value of the ratio $(e-e)_c/e''$ is 0.031, which is in approximate agreement with the value 0.038 observed.

The coincidence rate for the preceding photons and delayed radiation $(e'-q'')_d$ was then computed. For this the counting efficiency for photons was assumed to be independent of energy and has been called E''_q. This assumption should not be too seriously in error, since theoretical calculations indicate that counter photon efficiencies pass through a minimum in the region of interest.[17] Thus,

$$(e'-q'')_{d-\text{tot}}=\frac{n_9\omega'E_q''}{(1+\alpha_x)}\left[\frac{\alpha_9A_9'}{(1+\alpha_9)}+\frac{0.4n_{10}\alpha_{10}A_{10}'}{(1+\alpha_{10})n_9}+\frac{0.4n_{11}\alpha_{11}A_{11}'}{(1+\alpha_{11})n_9}+\frac{(n_9-0.4n_{11})\alpha_{4L}A_{4L}'}{n_9(1+\alpha_4)}\right]=n_9E_q''0.046. \quad (9)$$

The total photon counting rate is given by:

$$q''=n_9E_q''\left\{\frac{(n_4+n_{11})}{n_9(1+\alpha_x)}+\sum_i\frac{n_i}{n_9(1+\alpha_i)}\left[\frac{\alpha_{iK}}{(1+\alpha_x)}+1\right]\right\}=n_9E_q''9.5. \quad (10)$$

The $(e'-q'')/q''$ ratio for decay scheme A should be equal, therefore, to 0.0048, which is in serious disagreement with the experimental value of 0.051.

The high intensity assigned to gamma-ray 4 from spectrometer data requires it to be a transition to the ground state. The high experimental value of $(e'-q'')_{d-\text{tot}}/q''$ is incompatible with such a high intensity for this transition. Since the samples used in the spectrometer must be considered as thick with regard to the low energy electron ranges, large and uncertain corrections were required in order to calculate intensities. Accordingly, decay scheme B shown in Fig. 13 was considered also. In this case, transition 4 was placed before the metastable state and could not have an intensity greater than n_9. Its intensity was assumed to be this maximum value; and, in addition, the intensity of n_6 from a visual comparison of the peaks in Figs. 4 and 5 was taken as 0.5 n_9. The metastable state was chosen as the one at 376 kev following transition 4 and preceding transition 9. It should be noted that these calculations used the spectrometer intensity ratios e_{10}/e_9 and q_{10}/q_9 which were known most accurately, since the transition energies are not greatly different. In addition, the quantities, $(e_i/e_9)(q_9/q_i)$, were used for estimating some of the conversion coefficients. However, in these terms the energy dependence should largely cancel. In this case the electron counting component is taken as

$$\lim_{A''\to 1}e''=n_9\omega''\left[\frac{\alpha_{10}n_{10}}{(1+\alpha_{10})n_9}+\frac{\alpha_9}{(1+\alpha_9)}+\frac{\alpha_{4L}}{(1+\alpha_4)}+\frac{0.5\alpha_6}{(1+\alpha_6)}\right]\sim 1.9n_9\omega''\alpha_9/(1+\alpha_9). \quad (11)$$

TABLE IV. Decay scheme A. Relative intensities and conversion coefficients for gamma-rays.

Gamma-ray	Relative intensity	Conversion coefficient
	$(e_i+q_i)/(e_9+q_9)$	α_i
4	3.0	1.6
6	1.3	0.2
9	1.0	0.8
10	1.3	0.4
11	0.4	0.04

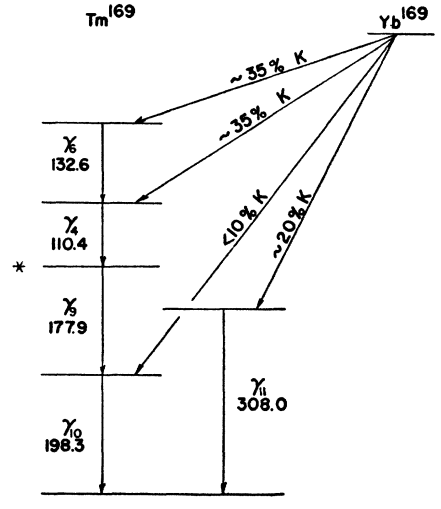

FIG. 13. Decay scheme B. The energies are given in kev.

[17] G. V. Drose, Z. Physik **101**, 474 (1937).

TABLE V. Decay scheme B. Relative intensities and conversion coefficients for gamma-rays.

Gamma-ray	Relative intensity	Conversion coefficient
	$(e_i+q_i)/(e_9+q_9)$	α_i
4	1.0*	3
6	0.5*	0.3
9	1.0	1.6
10	1.1	0.7
11	···	0.08

* Assumed values.

The electron–electron coincidence rate is

$$\lim_{A''\to 1}(e-e)_c=\frac{n_9\omega'\omega''\alpha_9\alpha_{10}(A_9'+A_{10}')}{(1+\alpha_9)(1+\alpha_{10})}. \quad (12)$$

From the experimental value of the ratio of $(e-e)_c/e''=0.038$ and the values of A_9', A_{10}', and ω' used previously, the value of $\alpha_{10}=0.7$ is obtained directly. Other conversion coefficients were computed from the data in Table III by means of the expression

$$\alpha_i=\alpha_{10}(e_i/e_{10})(q_{10}/q_i). \quad (13)$$

The results for decay scheme B are listed in Table V. The rate of the $(e'-q'')_{d-\text{tot}}$ coincidences can be computed from these values by the expression

$$(e'-q'')_{d-\text{tot}}=n_9E_q''\omega'\left[\frac{\alpha_9A_9'}{(1+\alpha_9)}+\frac{\alpha_{10}A_{10}'}{(1+\alpha_{10})}\right]\times\left\{\frac{1}{(1+\alpha_x)}+\frac{n_4}{n_9(1+\alpha_4)}\left[1+\frac{\alpha_{4K}}{1+\alpha_x}\right]+\frac{n_6}{n_9(1+\alpha_6)}\left[1+\frac{\alpha_{6K}}{(1+\alpha_x)}\right]\right\}. \quad (14)$$

The total observed photon count is given by

$$q''=n_9E_q''\left\{\frac{n_{10}}{n_9(1+\alpha_x)}+\sum_i\frac{n_i}{n_9(1+\alpha_i)}\left[1+\frac{\alpha_{iK}}{(1+\alpha_x)}\right]\right. \quad (15)$$

Substituting the values of Table V in these expressions gives an estimate of 0.048 for $(e'-q'')_{d-\text{tot}}/q''$, which is in very satisfactory agreement with the experimental value of 0.051. This agreement has resulted because the number of photons preceding the metastable state has been increased by the contribution from transitions 4 and 6. In decay scheme B there would appear to be no possible way to include transition 11 except as a separate branch for the orbital capture. A number of the other low intensity transitions will not fit into the B level scheme. It should be noted that scheme A employed all of the gamma-rays observed. It would be interesting to have these gamma-ray energies measured with a curved crystal spectrometer of high resolution as described by DuMond.[18] It would seem that contradictions between the results from the spectrometer and the coincidence experiments might be satisfactorily resolved by the use of a double beta-ray spectrometer with coincidence counting of the type described by Feather, Kyles and Pringle.[19]

In decay scheme B the metastable state decays by the emission of only one intense gamma-transition. The evidence indicates that this transition is most likely γ_9; however, the difference in intensities as indicated in Table V does not prevent the possibility of transition 10 preceding 9. The conversion coefficient of 1.6 for gamma 9 indicates that the radiation is probably magnetic 2^1 or 2^2 or electric 2^4.[20] The calculated ratios of e_K/e_L for magnetic 2^1 or 2^2 and electric 2^4 are 8, 7, and 0.3, respectively.[21] Hence, the radiation would not likely be electric 2^4. The calculated half-lives for magnetic dipole and quadrupole radiations with a conversion coefficient of 1.6 are 5.4×10^{-4} and 267 μsec, respectively, compared with our experimental value of 0.7 μsec.[22] This evidence indicates that magnetic quadrupole radiation is the most likely. With the conversion coefficient of α_{10} equal to 0.8, its radiation is probably magnetic dipole. In the reversed case in which gamma 10 precedes gamma 9 and would be the delayed transition, the γ_{10} half-life was calculated to be 174 μsec for magnetic quadrupole and 4.5×10^{-4} μsec for magnetic dipole.

For decay scheme A the metastable state must decay by three alternative transitions and the information for one of these is very incomplete.

The authors wish to express their appreciation to Dr. L. J. Laslett, Dr. W. W. Pratt, and Mr. G. O. Pickens for their assistance in obtaining part of the data, to Mr. E. R. Rathbun, Jr. for construction of the G-M counters used in the spectrometer, and to Mr. J. H. Jonte and Miss D. Christian for some of the chemical operations.

[18] J. W. M. DuMond, Rev. Sci. Instr. **18** 626 (1947).
[19] Feather, Kyles, and Pringle, Proc. Phys. Soc. (London) **61**, 466 (1948).
[20] Rose, Goertzel, Spinard, Han, and Strong, tables distributed privately.
[21] M. H. Hebb and E. Nelson, Phys. Rev. **58**, 486 (1940).
[22] E. Segrè and A. C. Helmholtz, Revs. Modern Phys. **21**, 271 (1949).